COMPDYN 2013
4th ECCOMAS Thematic Conference on
Computational Methods in Structural Dynamics and Earthquake Engineering
M. Papadrakakis, V. Papadopoulos, V. Plevris (eds.)
Kos Island, Greece, 12–14 June 2013

ROCKING RESPONSE OF SLENDER, FLEXIBLE COLUMNS UNDER PULSE EXCITATION

Michalis F. Vassiliou[1], Kevin R. Mackie[2] and Božidar Stojadinović[1]

[1]Institute of Structural Engineering (IBK), Swiss Federal Institute of Technology (ETHZ),
Wolfgang-Pauli-Strasse 15, 8093, Zürich, Switzerland
email: vassiliou@ibk.baug.ethz.ch and stojadinovic@ibk.baug.ethz.ch

[2]University of Central Florida,
Civil Environmental and Construction Engineering Department, Engr II 402, 4000 Central Florida Blvd., Building 91, Suite 211, Orlando, Florida 32816-2450
email: kmackie@mail.ucf.edu

Keywords: Rocking, Earthquake Engineering, Seismic Isolation

Abstract. *Early studies of the response of rigid blocks allowed to uplift and rock under seismic motion have shown a scale effect that characterizes the response of rocking blocks subjected to a ground motion. Namely; larger objects need a larger ground acceleration to overturn; and longer dominant period earthquakes have a larger overturning capability than shorter period ones. This is why it has been proposed that rocking can be used as an isolation strategy. However, actual structures are not rigid: structural elements where rocking is expected to occur are often slender and flexible. Modeling rocking of flexible bodies is a challenging task. A finite element model of a rocking elastic body that does not involve explicit modeling of impact is presented in this paper. This model was validated by comparing its response to pulse excitation with an analytical solution. It is concluded that the extensively studied rigid rocking block model provides a good approximation of the seismic response of an elastic rocking column for small-size columns and that it provides a conservative response estimate for larger columns. Guidance for development of rocking column models in ordinary finite element software is provided.*

1 INTRODUCTION

Early studies of the response of rigid blocks allowed to uplift and rock under seismic motion have been presented by Milne [1]. Housner [2] has shown a scale effect that characterizes the response of rocking blocks subjected to a ground motion: a) Larger objects need a larger ground acceleration to overturn b) Longer period earthquakes have a larger overturning capability than shorter period ones. For pulse-like records, the above results are presented in the form of rocking spectra in the papers by Zhang and Makris [3] and Makris and Konstantinidis [4]. In the latter paper it is shown that the representation of a rigid rocking block as a SDOF linear elastic system, a representation adopted by building codes (FEMA 356) is fundamentally flawed. In the present paper, it is shown that rigid rocking blocks can be modeled as SDOF nonlinear-elastic viscously-damped systems. This modeling makes possible the use ordinary FEM software equipped with nonlinear elastic elements and with nonlinear geometry capabilities to model the rocking response not only of rigid but of flexible blocks as well. Hence it can be used to study the influence of flexibility on the response of rocking structures, a phenomenon that has been examined by Psycharis [5], Olivetto et al. [6], Apostolou et al. [7] and recently by Acikgoz and DeJong [8]. The interest on the influence of the flexibility of structures on their rocking behavior originates from the studies on the feasibility of using rocking as an isolation technique with small residual displacements (Apostolou et al. [7], Gelagoti et al [9], Makris and Vassiliou [10]). It is worth mentioning that a bridge that uses rocking as an isolation technique has already been built in the Rangitikei river in New Zealand in 1981 (Beck and Skinner [11]). Moreover, it has been shown that ancient columns have survived earthquakes for more than 2,500 years due to their ability to sustain rocking motion without overturning (Konstantinidis and Makris [12])

2 REVIEW OF THE ROCKING RESPONSE OF A RIGID BLOCK.

With reference to Figure 1 (top left) and assuming there is no sliding, the equation of motion of a free standing block with size $R=\sqrt{h^2+b^2}$ and slenderness α=atan(b/h) subjected to a horizontal ground acceleration $\ddot{u}_g(t)$, when rocking around O and O' respectively is (Yim et al. [13], Makris and Roussos [14], Zhang and Makris [3], among others)

$$I_o\ddot{\theta}(t)+mgR\sin\left[\alpha\,\mathrm{sgn}\,\theta(t)-\theta(t)\right]=-m\ddot{u}_g(t)R\cos\left[\alpha\,\mathrm{sgn}\,\theta(t)-\theta(t)\right] \qquad (1)$$

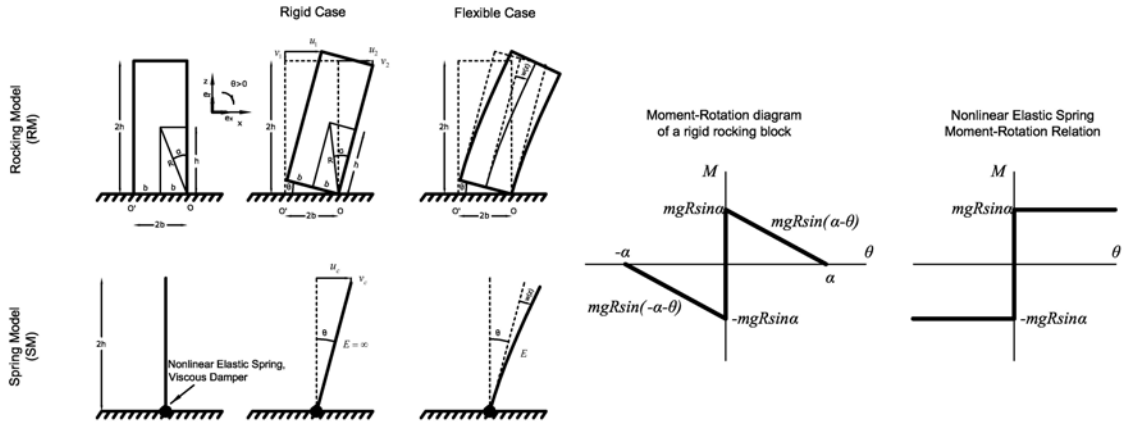

Figure 1. Left: Original Rocking Model (RM) and proposed Spring Model (SM). Right: Moment-rotation diagram of a rigid rocking block with slenderness α and size R; and Moment-Rotation relationship of the non linear elastic spring (unloads on the same path) used in the Spring Model.

For rectangular blocks, $I_o = (4/3)mR^2$ and the above equations can be expressed in the compact form

$$\ddot{\theta}(t) = -p^2 \left\{ \sin\left[\alpha \operatorname{sgn}\left(\theta(t)\right) - \theta(t)\right] + \frac{\ddot{u}_g}{g} \cos\left[\alpha \operatorname{sgn}\left(\theta(t)\right) - \theta(t)\right] \right\} \tag{2}$$

where $p = \sqrt{3g/4R}$.

Figure 1 (Right) shows the moment-rotation relationship during the rocking motion of a free-standing block. The system has infinite stiffness until the magnitude of the applied moment reaches the value $mgR\sin\alpha$, and once the block is rocking, its restoring force decreases monotonically, reaching zero when $\theta = \alpha$. This negative stiffness, which is inherent in rocking systems is most attractive in earthquake engineering in terms of keeping base shears and moments low (Makris and Konstantinidis [4]) provided that the rocking block remains stable.

During the oscillatory rocking motion, the moment-rotation curve follows the curve shown in Figure 1 (Right) without enclosing any area. Energy is lost only during impact, when the angle of rotation reverses. Conservation of angular momentum an instant before the impact and immediately after the impact gives:

$$r = \frac{\dot{\theta}_2^2}{\dot{\theta}_1^2} = [1 - \frac{3}{2}\sin^2\alpha]^2 \tag{3}$$

3 SDOF NONLINEAR ELASTIC VISCOUSLY DAMPED RIGID EQUIVALENT SYSTEM

Equations (2) and (3) can be easily solved with a numerical computing package (e.g. MATLAB [15]). However, the equations of more complex rocking structures or flexible rocking structures become much more complicated and their solution becomes cumbersome. Therefore, an equivalent SDOF nonlinear elastic viscously damped Spring Model (SM) is proposed (Figure 1). In this section the proposed Spring Model will be tested via a comparison with rigid rocking blocks and in the next section it will be used to examine the rocking behavior of finite stiffness columns.

The proposed model consists of a cantilever vertical column with crossection identical to the crossection of the rocking block connected to a nonlinear elastic spring (that unloads on the same path that it loads) with yield moment equal to *mgRsin(α)*, yield rotation tending to zero and zero post yielding stiffness (Figure 1) in parallel with a viscous damper with damping coefficient *c*. Note that in order for the two models to be equivalent (softening moment-rotation behavior after yield) *P-Δ* effects and large displacements should be taken into account. When the Spring Model is tested against the Rocking Model (RM) (i.e. the numerical solution of equation (2)), the young modulus, *E*, of the column material is taken very large so that the column does not bend.

The proposed Spring Model can be easily implemented in FEM software like OpenSees [16] or commercial products.

3.1 Comparison of the equations of motion

The equation of motion of the Spring Model (not taking into account damping) is

$$I_o'\ddot{\theta}(t) + mgR\left(\sin\alpha \operatorname{sgn}\theta - \cos\alpha \sin\theta\right) = -m\ddot{u}_g R\cos\alpha\cos\theta \tag{4}$$

where

$$I_o' = \frac{4}{3} mR^2 \cos^2 \alpha \tag{5}$$

Assuming $\cos\theta \simeq 1$ and $\sin\alpha \sin\theta \ll 1$, the equation of motion of a rigid rocking block (equation (1)) reduces to

$$I_o \ddot{\theta}(t) + mgR\left(\sin\alpha \operatorname{sgn}\theta - \cos\alpha \sin\theta\right) = -m\ddot{u}_g R \cos\alpha \cos\theta \tag{6}$$

If α is small, $\cos^2 \alpha \to 1$ and equations (4) and (6) become identical.

The moment of inertia appearing in equation (1) refers to rotational moment around the pivot point ($I_o = \frac{4}{3} mR^2$). However, assigning just translational masses in the FEM implementation of the spring model, give a moment of inertia given by equation (5). For this reason the Spring Model is enhanced by evenly distributing the difference $\Delta I_o = \frac{4}{3} mR^2 \left(1 - \cos^2 a\right)$ between all the rotational degrees of freedom of the vertical column. Initially assuming zero damping for both models, Figure 2 (left) plots time histories (obtained with OpenSees) of the response of a rigid (E=10^{11}kPa) block with height 2h=10m, and tanα=0.1, 0.2 and 0.3, when excited by a symmetric Ricker [17] pulse excitation with a_p = 4$g$tanα and ω_p=2π rad/s (Figure 2 – bottom). No damping is included in either of the models. The results show good agreement of the two methods.

3.2 Treatment of energy dissipation

Energy dissipation in rocking blocks takes place instantaneously at each impact. On the contrary the proposed model is equipped with a viscous damper at its base, a damping mechanism that dissipates energy continuously. However, viscous damping models are widely used to describe different kinds of energy dissipation (as long as it is not large). For example, the opening and closing of cracks in concrete, an energy dissipation mechanism that is similar to the mechanism of rocking, is widely modeled with viscous damping. This is why even though these two energy dissipation mechanisms act differently, this paper attempts to match the two dissipating mechanisms in terms of maximum rotation of the system.

In order determine the appropriate value of the viscous damping coefficient and assuming that it would not strongly depend on the column flexibility (an assumption that needs to be verified either experimentally or by more sophisticated numerical models), energy loss during the free vibration both of the Rocking Model and of the Spring Model will be studied.

In the case of the Rocking Model the energy dissipation per cycle of free vibration is independent of the amplitude of vibration and is described by the restitution factor r. The ratio of the energy after one complete cycle, E, to the initial energy, E_o, is

$$\frac{E}{E_o} = r^2 = \left(1 - \frac{3}{2}\sin^2 \alpha\right)^4 \tag{7}$$

Accordingly, for the Spring Model and for initial conditions $\theta(0) = \theta_o$ and $\dot{\theta}(0) = 0$ the corresponding ratio, ξ, is a function of 6 variables:

$$\frac{E}{E_o} = \xi = f\left(m, \alpha, R, g, \theta_o, c\right) \tag{8}$$

Each term of equation (8) includes only 3 reference dimensions ($\xi \doteq []$, $\alpha \doteq []$, $R \doteq [\mathrm{L}]$, $g \doteq [\mathrm{LT}^{-2}]$, $\theta_o \doteq []$, $c \doteq [\mathrm{ML}^2\mathrm{S}^{-1}]$). Hence, according to Buckinghams's Π theorem of dimensional analysis [18], equation (8) can be transformed into

$$\frac{E}{E_o} = \xi = \varphi\left(\frac{\theta}{\alpha}, \alpha, \frac{c}{mg^{0.5}R^{1.5}}\right) \tag{16}$$

Figure 3 plots Equation (9) for $0<\theta/\alpha<1$, $\tan\alpha = 0.1$, 0.2 and 0.3, and $\frac{c}{mg^{0.5}R^{1.5}}$=0.02, 0.08 and 0.18 respectively. The plot shows that a) The value of α is immaterial to ξ and b) that for $\theta/\alpha>0.5$, ξ only lightly depends on θ/α. Hence for $\theta/\alpha>0.5$ and $\alpha<0.3$, equation (16) reduces to

$$\frac{E}{E_o} = \xi = \varphi\left(\frac{c}{mg^{0.5}R^{1.5}}\right) \tag{10}$$

Equations (7) and (10) indicate that by equating the energy loss in a free vibration, a relation between $\frac{c}{mg^{0.5}R^{1.5}}$ and α can be determined so that the energy losses during a free vibration cycle of the two models is the same (at least for $\theta/\alpha>0.5$). Based on Figure 3, an analytical approximation would be

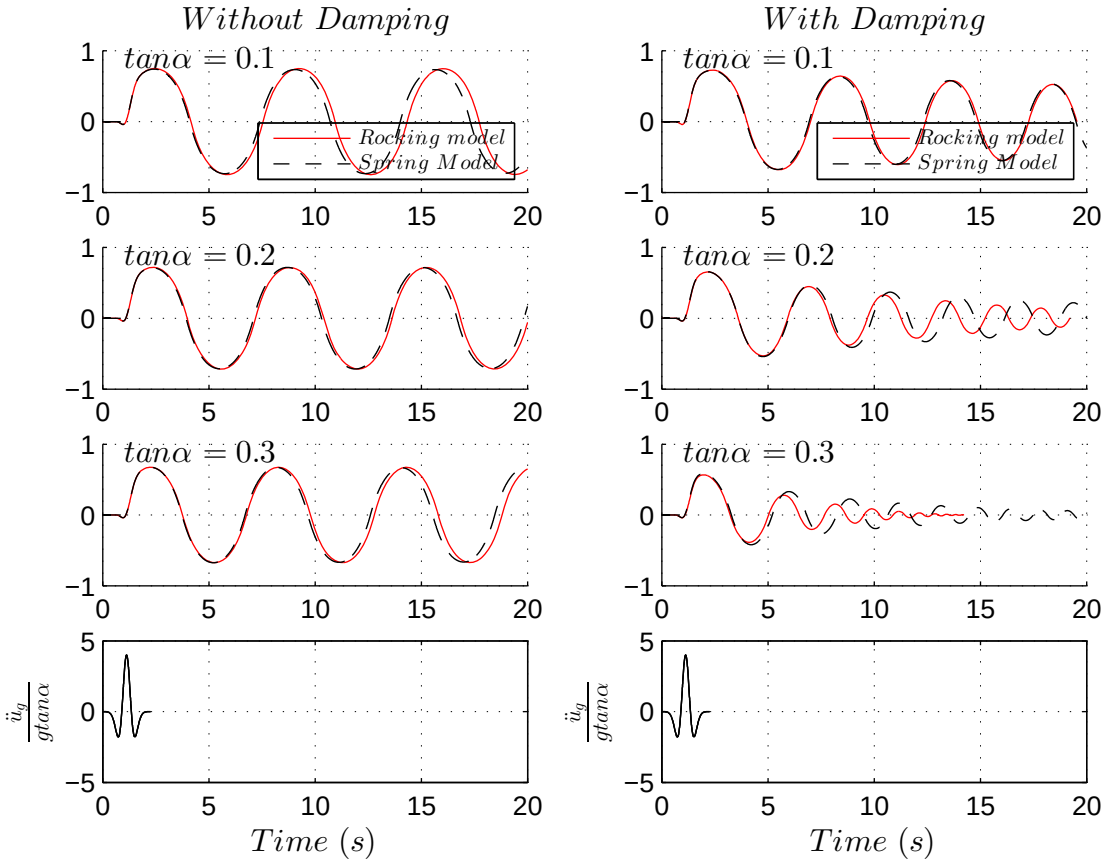

Figure 2. Time histories of the response of a rigid block with height 10m and slenderness tanα=0.1, 0.2 and 0.3 (top 3 rows), when excited by a symmetric Ricker pulse excitation with $a_p = 4g\tan\alpha$ and $\omega_p=2\pi$ rad/s (bottom row). The response was computed with the Rocking Model (RM) and the Spring Model (SM).

$$\frac{c}{mg^{0.5}R^{1.5}} = 0.02\left(\frac{\alpha}{0.1}\right)^2 \tag{11}$$

ElGawady et al. [19] have shown that the energy dissipation at every impact not only depends on slenderness, α, but it strongly depends on the interface material as well. Therefore the exact correlation of the damping of the two models is inherently non feasible and further investigation should be performed to correlate the damping coefficient to the real model taking into account the interface material.

Figure 2 (right) plots time histories of the response to a symmetric Ricker [17] pulse excitation (damping included). In all cases the proposed model is able to accurately predict the maximum rotation of the base. For the most slender case ($\tan\alpha$=0.1) it is able to predict accurately the whole time history. Its inability to predict the whole time history for the least slender case ($\tan\alpha$=0.3) is due to the inherently sensitive highly nonlinear nature of the rocking problem: The period of free vibration depends on the amplitude of the motion. Hence a small error in the estimation of the amplitude leads to error in the prediction of the phase of the motion. Accordingly, Figure 4 plots the overturning spectra for the two models demonstrating the ability of the Spring Model (SM) to approximate well the results of the Rocking Model (RM).

4 EXTENTION TO FLEXIBLE SYSTEMS

Even though rocking of rigid structures has been studied extensively relatively few studies have been carried on the influence of the flexibility of a structure on its rocking behavior. This section attempts to shed light on the interaction of elasticity and rocking of flexible blocks and to examine the limits of the validity of the rigid block assumption. This is accomplished by extending the method developed in the previous section to study the behavior of flexible rocking columns. The model examined is shown in Figure 1. It is an Euler-Bernoulli beam (made out of a material with young modulus E and density ρ) that is allowed to uplift. Roh and Reinhorn [20] performed experiments on rocking concrete columns and proved that, for low values of axial force, spalling of concrete does not occur when the column uplifts. Therefore, it is reasonable to assume that, in the column examined in this section, the axial

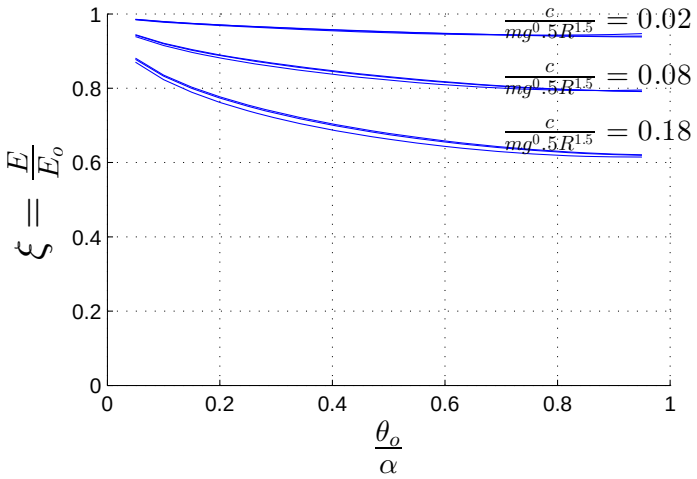

Figure 3 Damping ratio, ξ, plotted against the normalized initial angle of rotation θ_o/α for free vibrations of the Spring Model for different values of α and $\frac{c}{mg^{0.5}R^{1.5}}$.

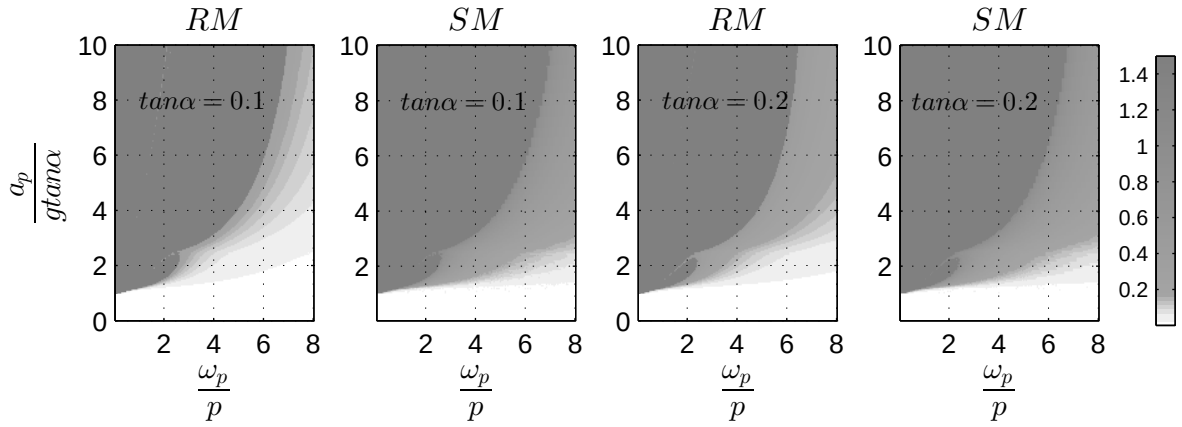

Figure 4 Contour plots of the maximum rotation of rigid blocks subjected to a symmetric Ricker pulse.

force of which is only due to its self weight, no spalling will occur and the column will rotate around points O and O'. Moreover, since the axial force is small, it is assumed that the curvature at the base of the column when rocking initiates will be negligible. In the presence of extra axial load this curvature might not be negligible and the yield rotation of the Spring Model should be adjusted accordingly. The damping ratio, ζ, is the damping ratio of the column prior to its uplift, i.e. The damping ratio for a fixed cantilever column.

4.1 Dimensional analysis of the system

The overturning instability of a flexible rocking column subjected to a symmetric Ricker pulse is described by its base rotation and is a function of 7 variables.

$$\theta(t) = f\left(a_p, \omega_p, g, R, \alpha, \zeta, \rho, E\right) \tag{12}$$

Each term of equation (12) includes only 3 reference dimensions ($a_p \doteq [\,LT^{-2}]$, $\omega_p \doteq [T^{-1}]$, $g \doteq [LT^{-2}]$, $R \doteq [L]$, $\alpha \doteq []$, $\zeta \doteq []$, $\rho \doteq [ML^{-3}]$, $E \doteq [ML^{-1}S^{-2}]$). Hence, according to Buckinghams's Π theorem of dimensional analysis [18], equation (12) can be transformed into

$$\theta(t) = \varphi\left(\frac{a_p}{g\tan\alpha}, \frac{\omega_p}{p}, \alpha, \zeta, \frac{E}{\rho g R}\right) \tag{12}$$

From the above equation it can be seen that the response of the column depends on the ratio *E/R*. Hence, it is expected that the flexibility of the columns will have a more significant effect on larger columns. Moreover, since for a specified material, the Young modulus, *E*, and the density, ρ, are constant, the dimensionless flexibility $\frac{E}{\rho g R}$ solely depends on the size of the column.

It is worth noting that, for specified material properties, *E* and ρ, and slenderness α, the first eigenperiod of the column before uplift depends only on its size

$$T_1 = 12.38\sqrt{\frac{\rho}{E}}\frac{h}{\tan\alpha} \tag{13}$$

The flexible rocking column is studied via the proposed FEM model by using a material with finite stiffness. Energy dissipation due to impact is modeled by the same type of viscous damper that was used for the rigid case. Energy dissipation inside the column is modeled by

applying Rayleigh damping only at the nodes of the column (an option available in OpenSees). This is because applying Rayleigh Damping to the whole the model would result in excessive overall damping due to the very large pre yielding stiffness of the spring used to model the rocking behavior.

Figure 5 plots the contour plots of the maximum rotation over slenderness, θ/α, at the base of a concrete column with Young modulus E=30GPa and density ρ=2.5Mg/m^3 subjected to a symmetric Ricker pulse of amplitude a_p and cyclic frequency ω_p. Since most of the energy dissipation occurs at the base of the rocking column, the damping ratio, ζ, of the cantilever column was set to 0.01. The response was computed using the Spring Model implemented in OpenSees.

Figure 6 plots the minimum overturning acceleration spectra (i.e. the minimum acceleration required to overturn the concrete column) for several values of slenderness and height. It also shows the acceleration required to uplift the column. The plots show that for columns with tanα>0.2, the flexibility of the column is immaterial to the overturning stability and the rigid model gives accurate results.

For smaller values of tanα, Figure 6 indicates that the flexibility of the concrete column decreases the acceleration needed to cause uplift to values less than $g$tanα. This is because, for the range of ω_p/p plotted, the eigenperiods of the concrete column fall in the spectral region where the spectral acceleration is larger than PGA. Concerning the minimum acceleration to overturn the column, Figure 6 shows that for ω_p/p<4.5 the concrete column is less stable than the rigid column while for ω_p/p>4.5 the concrete column exhibits superior stability. It is worth noting that for columns large enough for their flexibility to influence their rocking response, small values ω_p/p correspond to pulses with unrealistically large periods. Hence, flexibility becomes important only for the region where it is beneficiary to the response. Therefore it is concluded that the results of solitary rigid columns analysis are applicable to solitary concrete columns because they are either accurate (for small size columns) or at the safe side (for larger size columns).

In an attempt to examine the interaction of elasticity and rocking, Figure 7 plots the response of a rigid and a concrete column with dimensions $2h$=$50m$ and $2b$=$5m$ when excited by symmetric Ricker pulses with ω_p/p=3 (T_p=3.87s) and ω_p/p=6 (T_p=1.93s) and acceleration amplitude a_p/gtanα=2.6 (a_p=2.55m/s^2) and a_p/gtanα=5.85 (a_p=5.74m/s^2). The first row plots the normalized rotation at the base of the column, θ/α and the second row plots the flexural deformation at the top of the column, w, i.e. the difference between the total top displacement and the top displacement due to base rotation. The plot indicates that at each impact the deformation at the top caused by flexure reverses. This reversal generates flexural vibration at the column. Hence, part of the rotational kinetic energy of the column is transformed into high frequency flexural vibration energy, which cannot cause the column to overturn. This transformation is the reason for which the concrete is more stable than the rigid column for ω_p/p=6 (left). On the contrary, for the case where ω_p/p=3 (right) the pulse has a smaller amplitude and the first part of it only slightly lifts the column. Therefore, the flexural vibration caused by the impact is less intense and most of the rotation kinetic energy is conserved.

Note that the flexural vibration has a much higher frequency than the column's eigenfrequency and is more heavily damped than what ζ=0.01 would indicate. This behavior is in accordance to the findings of Acikgoz and DeJong [8] for a SDOF oscillator able to uplift.

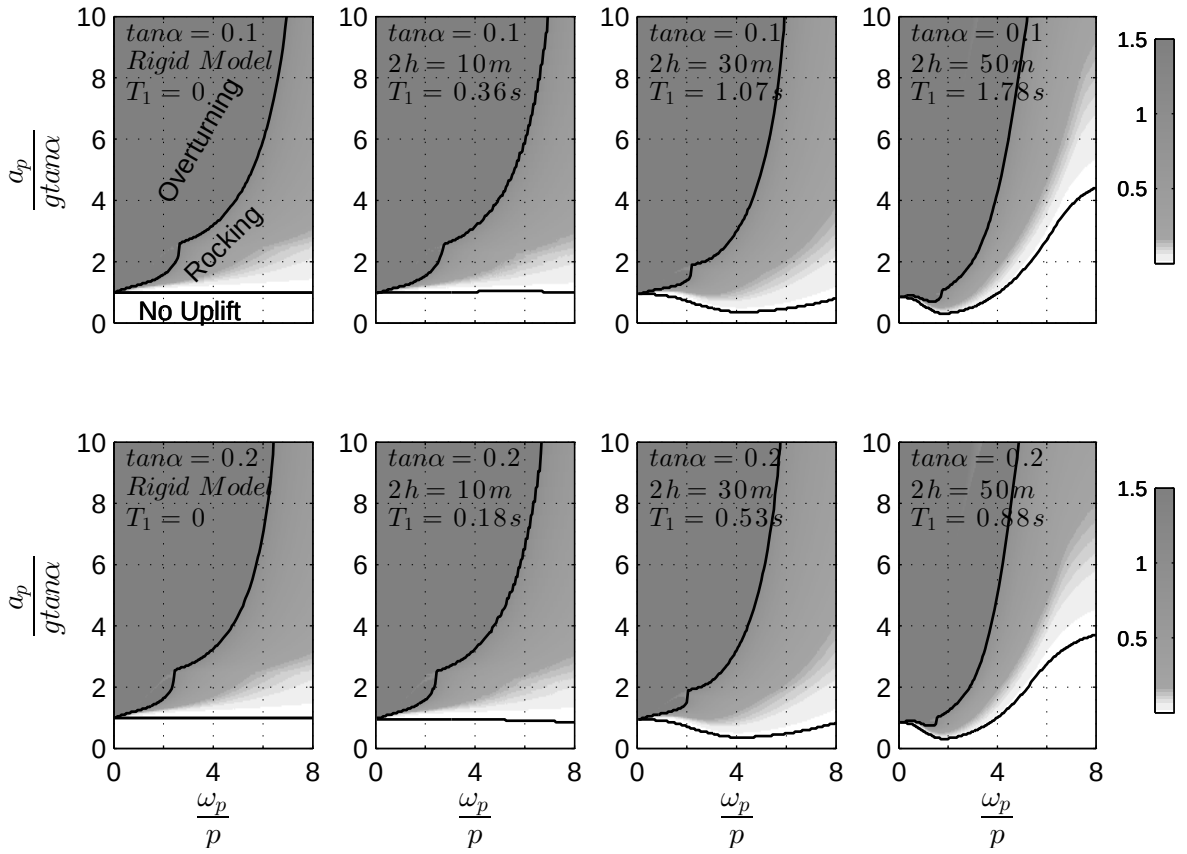

Figure 5 Contour plots of the normalized rotation, θ/α, of concrete (E=30GPa, ρ=2.5Mg/m^3) columns with height 2h and slenderness α when subjected to a symmetric Ricker acceleration pulse with amplitude a_p and cyclic frequency ω_p. The bold lines define the margin between uplift and no-uplift regions as well as the minimum acceleration to cause overturn.

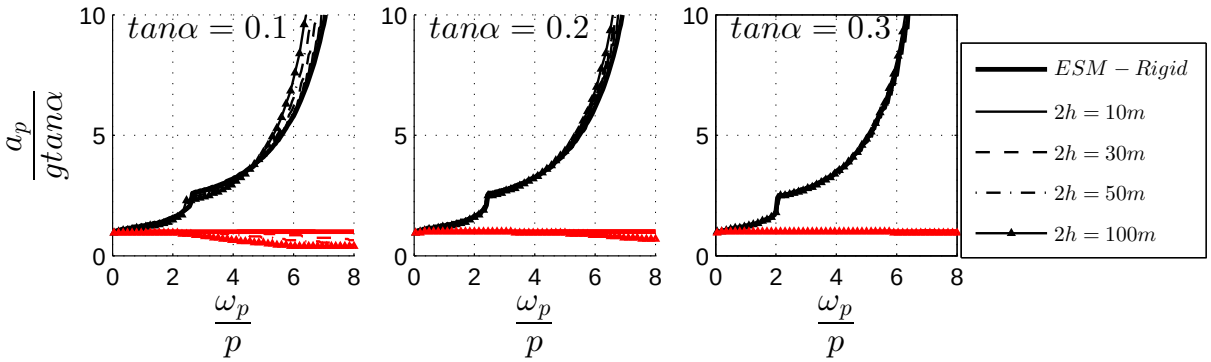

Figure 6 Minimum uplift and overturning acceleration spectra of concrete (E=30GPa, ρ=2.5Mg/m^3) columns with height 2h and slenderness α when subjected to a symmetric Ricker acceleration pulse with amplitude a_p and cyclic frequency ω_p.

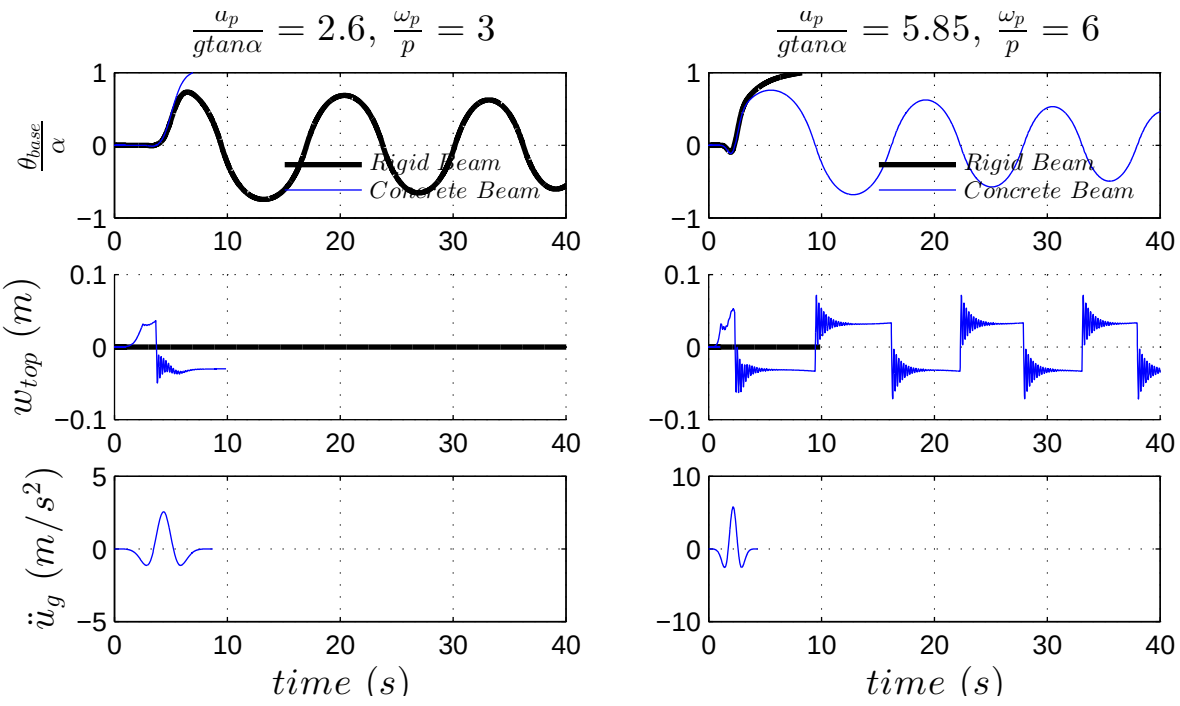

Figure 7 Comparison of time histories of the response of a rigid and a concrete beam of slenderness α and frequency parameter p, when subjected to a symmetric Ricker pulse with amplitude a_p and cyclic frequency ω_p. First row: normalized base rotation; Second row: top displacement due to bending; Third row: Ground acceleration

5 ROCKING OF COLUMNS OF FINITE STIFFNESS ON A RIGID BASE

In the usual design approach the column dimensions are based on their section forces capacity – not on their rocking stability. The latter is ensured by monolithically connecting the column to a large enough foundation. The foundation is designed so that no uplift occurs. This constraint often requires a very large foundation that makes the column behave like a fixed base one, thus transmitting large forces to the structure. It has been proposed [9, 20-23] that the foundation should be allowed to uplift or that the ground should be allowed to reach its bearing capacity so that the forces transmitted to the structure become smaller. This approach leads to lighter structures but the mobilization of all the soil strength often leads to large residual displacements, which is an undesirable performance. Makris and Vassiliou [10] have shown that frames consisting of unconnected assemblies of rigid bodies experience remarkable stability with zero residual deformations and suggested that uplift and rocking can be used as seismic isolation strategy strategies. When it comes to applying this concept to a sole rocking column (e.g. a tall chimney) the foundation and the column can be designed based on the ground acceleration that the designer would choose to cause uplift. In this section, the response of flexible rocking columns connected to a rigid foundation able to uplift is studied. It is investigated whether the increase in the flexural deformation prior to uplift due to the presence of the foundation makes the flexibility of the column influence the response of the system. The system that is studied is shown in Figure 8.

The equation of motion for the case where the column is rigid is

$$\ddot{\theta}(t) = -p'^2\left\{\sin\left[\alpha'\,\mathrm{sgn}\left(\theta(t)\right) - \theta(t)\right] + \frac{\ddot{u}_g}{g}\cos\left[\alpha'\,\mathrm{sgn}\left(\theta(t)\right) - \theta(t)\right]\right\} \tag{14}$$

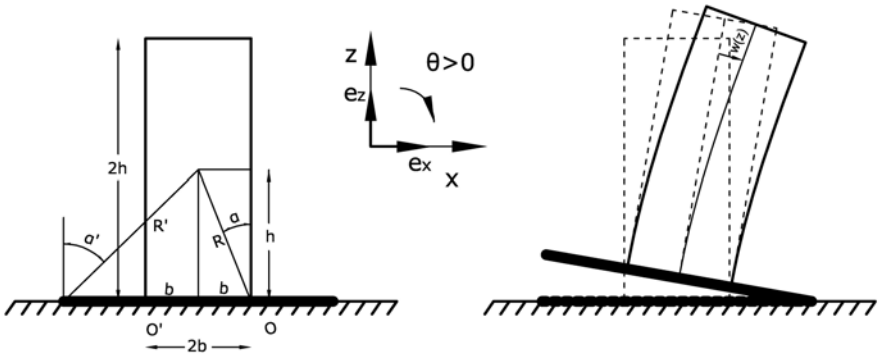

Figure 8 Flexible beam monolithically connected to a rigid base.

where

$$p'^2 = \frac{mgR'}{I'_o} \tag{15}$$

where α' and R' are defined in Figure 8 and I'_o is the moment of inertia of the rocking system around the pivot point and is equal to

$$I'_o = \frac{1}{3}mR^2 + mR^2\frac{\cos\alpha}{\cos a'} \tag{16}$$

Equations (15) and (16) give

$$p'^2 = p^2\frac{4\cos\alpha}{3\cos\alpha + \cos\alpha'} \tag{17}$$

that gives $p \simeq p'$ for small α and α'.
The uplift acceleration is

$$\ddot{u}_g^{uplift} = g\tan\alpha' \tag{18}$$

and the restitution coefficient is

$$r' = \left(1 - \frac{3}{2}\sin^2 a'\frac{\cos^2\alpha}{\cos\alpha'}\frac{4}{\cos\alpha' + 3\cos\alpha}\right)^2 \tag{19}$$

that gives $r' \simeq r = \left(1 - \frac{3}{2}\sin^2\alpha\right)^2$ for small α and α'.
Hence, if the column is rigid enough and for small α', columns with equal footing, $2b'$, and height, $2h$, behave the same, no matter what their width, $2b$, is.

In order for the Spring Model to be used to model this system in an ordinary FEM software the elastic nonlinear spring used at the base of the column should have a yield moment equal to $mgR'\sin\alpha'$. The extra rotational mass that should be distributed to the nodes of the model is $\Delta I = mR^2\left(\frac{1}{3} + \frac{\cos\alpha}{\cos\alpha'} - \frac{4}{3}\cos^2\alpha\right)$.

Extending equation (12), the overturning stability of a flexible column connected to rigid base is given by

$$\theta(t) = \varphi\left(\frac{a_p}{g \tan\alpha}, \frac{\omega_p}{p}, \alpha, \zeta, \frac{E}{\rho g R}, \alpha' \right) \tag{20}$$

Figure 9 plots the contour plots of the normalized maximum rotation, θ/α', at the base of a concrete column with Young modulus E=30GPa and density ρ=2.5Mg/m^3 subjected to a symmetric Ricker pulse of amplitude a_p and cyclic frequency ω_p. The response was computed using the Spring Model implemented in OpenSees. Figure 10 plots the overturning and uplifting minimum acceleration spectra for the same columns. Even in this case, where the developed moments are larger than in the column without a base, the effect of column flexibility is negligible for tanα>0.2. For columns with tanα=0.1, the flexibility of the column influences the response only for columns taller than 50m and for ω_p/p smaller than 4. For this size of columns, these values of ω_p/p correspond to unrealistic pulses with periods larger than 5 seconds. Therefore, it is concluded that Housnser's rigid model can be used to describe the rocking motion of columns with a slenderness as low as tanα=0.1 and a height of 100m, connected to a base 3 times larger than their width.

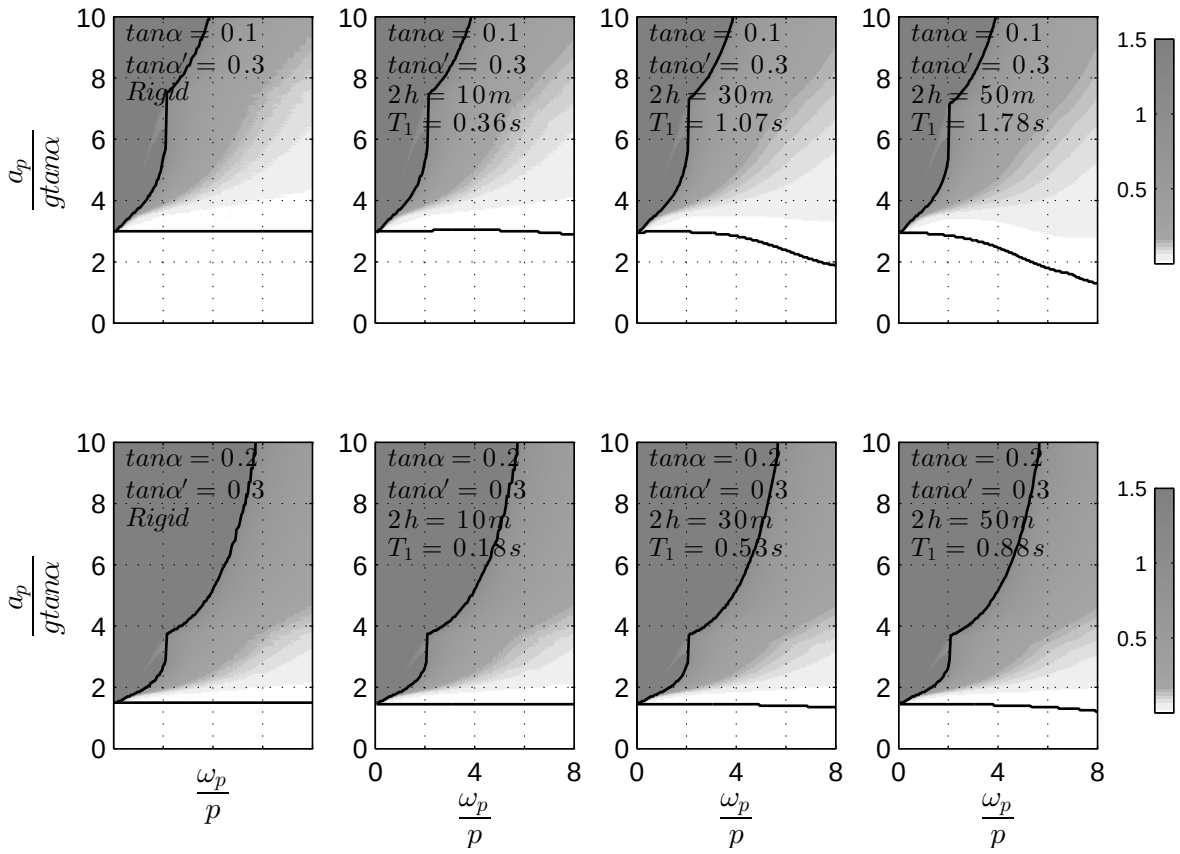

Figure 9 Contour plots of the normalized rotation, θ/α, of concrete (E=30GPa, ρ=2.5Mg/m^3) columns with height $2h$ and slenderness α connected to a rigid base with $\tan\alpha' = 0.3$, when subjected to a symmetric Ricker acceleration pulse with amplitude a_p and cyclic frequency ω_p. The bold lines define the margin between uplift and no-uplift regions as well as the minimum acceleration to cause overturn.

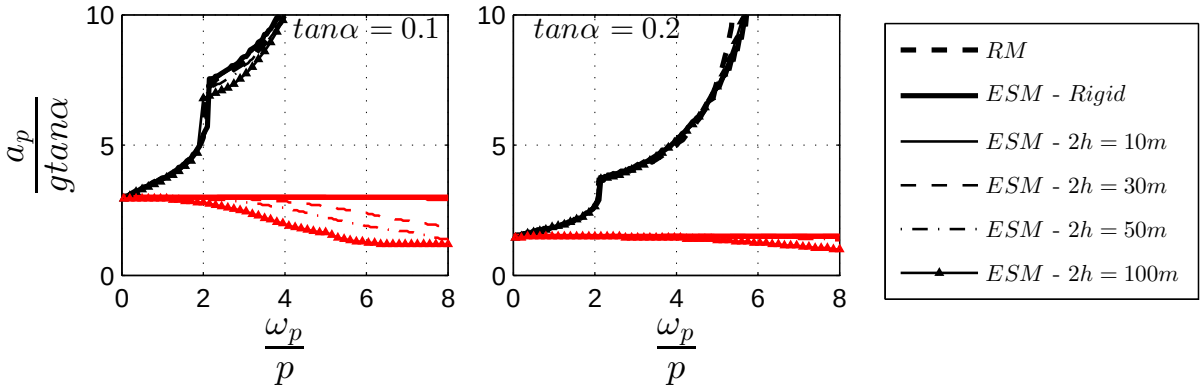

Figure 10 Minimum uplift and overturning acceleration spectra of concrete (E=30GPa, ρ=2.5Mg/m^3) columns with height $2h$ and slenderness α connected to a rigid base with $\tan\alpha' = 0.3$, when subjected to a symmetric Ricker acceleration pulse with amplitude a_p and cyclic frequency ω_p.

6 APPLICATION ON A ROCKING CHIMNEY

The use of rocking structures in construction dates back to ancient times. However, there is no historical evidence that ancient engineers actually designed rocking structures having in mind their rocking behavior during an earthquake. To the authors' knowledge, the first conscious uses of rocking as a seismic response modification mechanism were for a bridge across the Rangitikei river in New Zealand in 1981 (Beck and Skinner [11]) and for rocking chimney at the Christchurch airport (Sharpe and Skinner [24]).

The latter is a 33m tall chimney of cruciform cross section on a 7.5m×7.5m base. The chimney is designed so that it can rock during large earthquakes. Extra energy dissipation is provided by two steel hysteretic dampers. The chimney is equipped with an original system that allows the rocking motion, while preventing the chimney from walking off the foundation. Sharpe and Skinner mention that the chimney's "freedom to rock gives it the ability to withstand very large earthquakes without requiring the substantial repairs that most reinforced concrete structures would need".

In order to test the application of rocking motion as an isolation technique, the chimney is excited by the NS component of the ElCentro 18/5/1940 ground motion, which was used in the original paper by Sharpe and Skinner. To demonstrate the effectiveness of rocking, the chimney is modeled without the extra steel hysteretic dampers. For simplicity the cross section is modeled as constant across the height of the column with I_{xx}=I_{yy}=2.99m^4 and A=1.74m^2. Figure 11 plots the response histories of the chimney based a) on the original foundation and b) on a foundation large enough so that the chimney does not uplift: The rocking chimney develops a maximum base moment (M_{base}) of 7327 kNm while the fixed base one a maximum of 33200 kNm.

Hence the chimney and the foundation can be designed with less than a quarter of the moment that would develop if the column was designed not to uplift. The maximum rotation of the rocking column is as small as $0.036\,a'$ (i.e. less than 4% of the rotation that would cause overturning). Note that the second plot of Figure 11 shows that flexural deformation cannot be neglected and that modeling the chimney as a rigid block would give large error. This is due to the small radius of gyration (I/A) of the cruciform cross section.

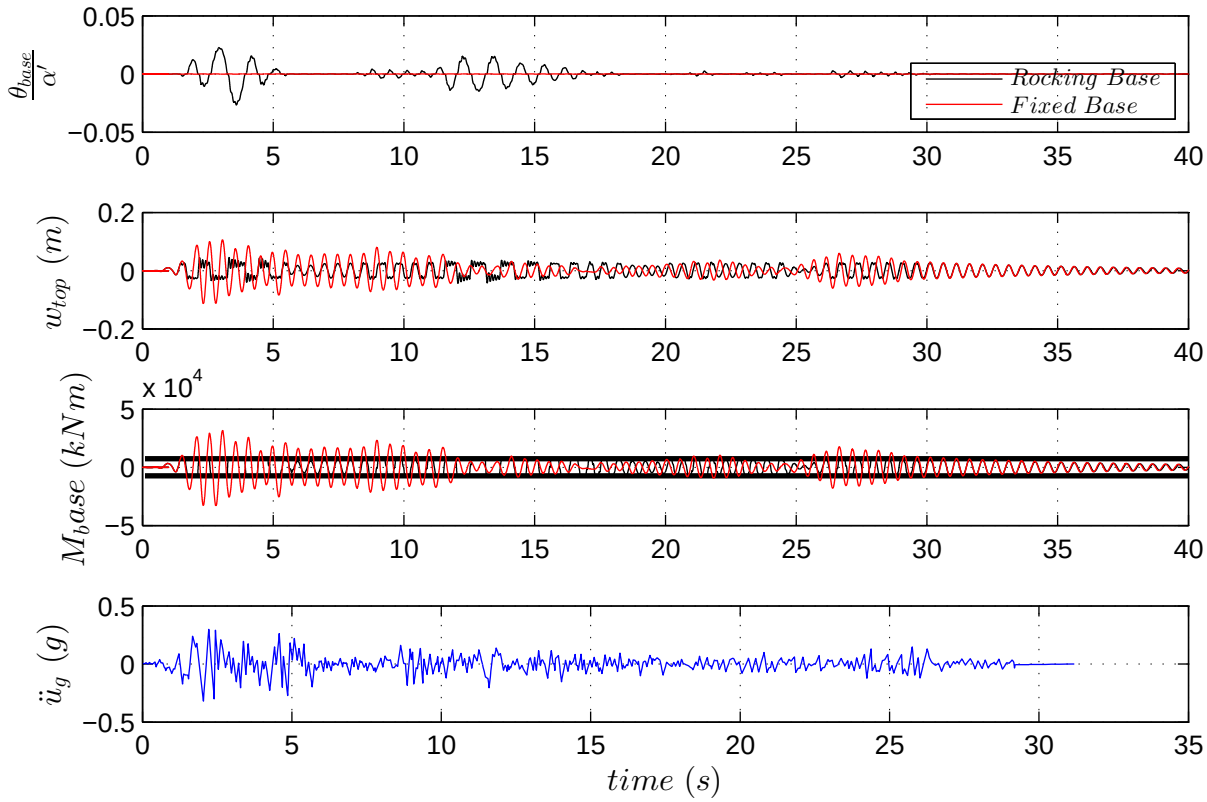

Figure 11 Response time histories of Sharpe and Skinner's chimney based a)on the original foundation and b) on a foundation large enough not to uplift First row: normalized base rotation; Second row: top displacement due to bending; Third row: Base moment Forth row: Ground acceleration (El Centro 18/5/1940 ground motion, NS Component)

7 CONCLUSIONS

A simple model for the description of rocking structures has been proposed. The model can be implemented in any FEM software that can handle large displacements, P-Δ effects and nonlinear elastic elements. Due to its simplicity, it takes so little computational time that it was able to produce rocking spectra. The model has been enhanced with extra rotational masses to take into account the minor effect of the fact that the real columns do not rotate around the center of their base but around its edge. The model was tested against the numerical solution of Housner's equation for rigid blocks with excellent results. Subsequently, it was used to study the effect of the flexibility of rocking solitary columns (with or without a base). It is concluded that for concrete rectangular columns the effect of their flexibility in their rocking response is negligible for columns up to 30m tall and on the safe side for taller columns. The latter is a result of the transformation of rotational kinetic energy to bending vibration at each impact. Finally the model was used to test the performance of an existing rocking chimney equipped with extra dissipation. It is concluded that the rocking chimney would exhibit remarkable stability even without the extra damping.

REFERENCES

1.Milne, J. (1885). ‘‘Seismic experiments.’’ *Trans. Seism. Soc. Japan*, 8, 1–82.

2.Housner, G. W. The behaviour of inverted pendulum structures during earthquakes. *Bulletin of the Seismological Society of America.* 1963; **53(2)**: 404–417.
3.Zhang J, Makris N. Rocking response of free-standing blocks under cycloidal pulses. *Journal of Engineering Mechanics*, ASCE 2001; 127(5):473–483.
4.Makris, N. and Konstantinidis, D. (2003), The rocking spectrum and the limitations of practical design methodologies. *Earthquake Engineering & Structural Dynamics*, 32, pp265–289.
5.Psycharis, I. N. and Jennings, P. C. (1983), Rocking of slender rigid bodies allowed to uplift. *Earthquake Engineering & Structural Dynamics*, 11: 57–76. doi: 10.1002/eqe.4290110106
6. Oliveto, G., Caliò, I. and Greco, A. (2003), Large displacement behaviour of a structural model with foundation uplift under impulsive and earthquake excitations. *Earthquake Engng. Struct. Dyn*., 32: 369–393.
7. Apostolou M, Gazetas G, Garini E. (2007) Seismic response of slender rigid structures with foundation uplifting, *Soil Dynamics and Earthquake Engineering*, 27(7), 642-654,
8. Acikgoz, S. and DeJong, M. J. (2012), The interaction of elasticity and rocking in flexible structures allowed to uplift. *Earthquake Engng. Struct. Dyn*.. doi: 10.1002/eqe.2181
9. Gelagoti, F., Kourkoulis, R., Anastasopoulos, I. and Gazetas, G. (2012), Rocking isolation of low-rise frame structures founded on isolated footings. *Earthquake Engng. Struct. Dyn*., 41: 1177–1197.
10. Makris N. and Vassiliou M.F. (2012), Planar rocking response and stability analysis of an array of free standing columns capped with a freely supported rigid beam (2012) *Earthquake Engng. Struct. Dyn* (accepted for publication).
11. Beck, J. L. and Skinner, R. I. (1973), The seismic response of a reinforced concrete bridge pier designed to step. *Earthquake Engng. Struct. Dyn*., 2: 343–358.
12. Konstantinidis, D. and Makris, N. (2005), Seismic response analysis of multidrum classical columns. *Earthquake Engng. Struct. Dyn*., 34: 1243–1270.
13. Yim CS, Chopra AK, Penzien J. Rocking response of rigid blocks to earthquakes. *Earthquake Engineering and Structural Dynamics* 1980; **8**(6):565–587.
14. Makris N, Roussos Y. Rocking response of rigid blocks under near-source ground motions. *Geotechnique* 2000; **50**(3):243–262
15. MATLAB Version 2011b. The Language of Technical Computing. The Mathworks, Inc.: Natick, MA, 1999.
16. OpenSEES (Open System for Earthquake Engineering Simulation), opensees.berkeley.edu
17. Ricker N. Further developments in the wavelet theory of seismogram structure (1943). *Bulletin of the Seismological Society of America*; 33:197–228.
18. Barenblatt, G. I. (1996), Scaling, self-similarity, and intermediate asymptotics, Cambridge University Press, Cambridge, U.K
19. ElGawady, M. A., Ma, Q., Butterworth, J. W. and Ingham, J. (2011), Effects of interface material on the performance of free rocking blocks. *Earthquake Engng. Struct. Dyn*., 40: 375–392.
20. Roh H., Reinhorn A., (2010) Modeling and seismic response of structures with concrete rocking columns and viscous dampers, *Engineering Structures*, 32(8), 2096-2107,
21. Pecker A, Pender MJ. (2000) Earthquake resistant design of foundations: new construction. Invited paper. GeoEng Conference, Melbourne 2000, 1:313–332.
22. Kawashima K, Nagai T, Sakellaraki D. (2007) Rocking seismic isolation of bridges supported by spread foundations. *Proc.of 2nd Japan-Greece Workshop on Seismic Design, Observation, and Retrofit of Foundations*, Tokyo, Japan 2007; 1:254–265.

23. Anastasopoulos I, Gazetas G, Loli M, Apostolou M, Gerolymos N. (2010) Soil failure can be used for earthquake protection of structures. *Bulletin of Earthquake Engineering*; 8:309–326.
24. Sharpe RD, Skinner RI, The seismic design of an industrial chimney with rocking base, (1983) *Bulletin of the New Zealand National Society for Earthquake Engineering* 16(2):98-106